Shaping solitons by lattice defects

Liangwei Dong[1,*] and Fangwei Ye[2]

[1]*Institute of Information Optics of Zhejiang Normal University, Jinhua 321004, China*

[2]*Department of Physics, Centre for Nonlinear Studies, and the Beijing-Hong Kong-Singapore Joint Centre for Nonlinear and Complex Systems (Hong Kong), Hoongkong Baptist University, Kowloon Tong, China*

(Received 15 April 2010; published 24 November 2010)

We demonstrate the existence of shape-preserving self-localized nonlinear modes in a two-dimensional photonic lattice with a flat-topped defect that covers several lattice sites. The balance of diffraction, defocusing nonlinearity, and optical potential induced by lattices with various forms of defects results in novel families of solitons featuring salient properties. We show that the soliton shape can be controlled by varying the shape of lattice defects. The existence domains of fundamental and vortex solitons in the semi-infinite gap expand with the defect amplitude. Vortex solitons in the semi-infinite gap with rectangular intensity distributions will break into dipole solitons when the propagation constant exceeds a critical value. In the semi-infinite and first-finite gaps, we find that lattices with rectangular defects can support stable vortex solitons which exhibit noncanonical phase structure.

DOI: 10.1103/PhysRevA.82.053829 PACS number(s): 42.65.Tg, 42.65.Jx, 42.65.Wi

I. INTRODUCTION

Optical wave propagation in periodic photonic structures displays unique phenomena that are absent in homogeneous media. Lattice solitons have drawn a great deal of attention in both fundamental physics and applications [1–3]. Thus far, diverse types of self-localized beams in optically induced lattices, such as fundamental [4], multipole [5,6], vortex [4,7–11], and necklace-like [12] solitons as well as gap soliton trains [13], have been predicted theoretically and observed experimentally in focusing and defocusing media. Periodic forcing can control and manage the localized states in two-dimensional dissipative systems [14].

Defects and defect states exist in a variety of linear and nonlinear systems, including solid state physics, photonic crystals, and Bose-Einstein condensates. If a periodic lattice has a local defect, this defect can affect the propagation of a probe beam in a fundamental way. Linear defect modes in one-dimensional (1D) [15,16] and two-dimensional (2D) [17,18] photonic lattices were investigated. Shallow defect states also exist near the edge of a band gap [19]. On the other hand, nonlinear localized modes bifurcating from linear defect modes in both attractive and repulsive defects were proven to be stable in certain parameter regimes [20]. Stable defect vector gap solitons [21] and surface-defect gap solitons [22] in 1D photonic lattices are also possible.

Very recently, properties of discrete solitons in optically induced photorefractive lattices with single-site and line defects were studied in [23]. Two-dimensional solitons located in defect channels at the surface of a hexagonal waveguide array were also observed [24]. The existence and stability of single-site defect solitons in 2D optical lattices imprinted in a photorefractive crystal were investigated [25]. Solitons in vacancy defects, edge dislocations, and quasicrystal structure were predicted by Ablowitz *et al.* [26]. A lower index core and a cylindrical core covering several lattice sites or rings were proposed to support 1D defect (kink) or 2D centrosymmetric solitons [27]. Nonlinear signal switching between two low-index defect channels is also possible [28].

Despite the above progress, defect solitons and their stability in a defect that covers several lattice sites are still poorly understood. Although nonlinear modes in multiple-site defects in both focusing and defocusing lattices were briefly addressed in [29], the shaping effects of defects on the solitons and the existence of vortex solitons have not yet been explored. Here, we study the properties of solitons supported by a 2D harmonic lattice with a flat-topped defect that covers several lattice sites in defocusing Kerr media. The main purpose of this article is twofold. First, we demonstrate that soliton shape can be controlled by the shape of lattice defects. Second, we find that defective lattices can support stable nonlinear modes (e.g., vortex solitons) in the semi-infinite gap in the defocusing media, which may not even exist in defect-free lattices.

II. MODEL

We consider beam propagation in a defocusing Kerr medium with an imprinted defective optical lattice governed by the nonlinear Schrödinger equation for normalized complex amplitude q:

$$i\frac{\partial q}{\partial z}+\frac{1}{2}\Delta q-|q|^2q+pR(x,y)q=0. \tag{1}$$

Here, $\Delta=\partial^2/\partial x^2+\partial^2/\partial y^2$, the transverse x,y and longitudinal z coordinates are scaled to the beam width and diffraction length, respectively, and p is the depth of the harmonic lattice. The function $R(x,y)$ characterizes the refractive index profile: $R(x,y)=\cos^2(\Omega x)+\cos^2(\Omega y)$ for $|x|>n_x\pi/(2\Omega),|y|>n_y\pi/(2\Omega)$, and $R(x,y)=\gamma(\gamma>0)$ otherwise, where Ω is the frequency, $n_{x,y}$ is the number of lattice periods covered by the flat-topped defect, and γ is the defect depth. When the defect is lower than the surrounding lattice sites ($\gamma<2p$), light tends to escape from the defect to nearby lattices sites. According to Ref. [20], we call such defects "repulsive defects." Conversely, an "attractive defect" forms when $\gamma>2p$. Such refractive index landscapes might be optically induced by properly imaging an amplitude mask with

*donglw@zjnu.cn

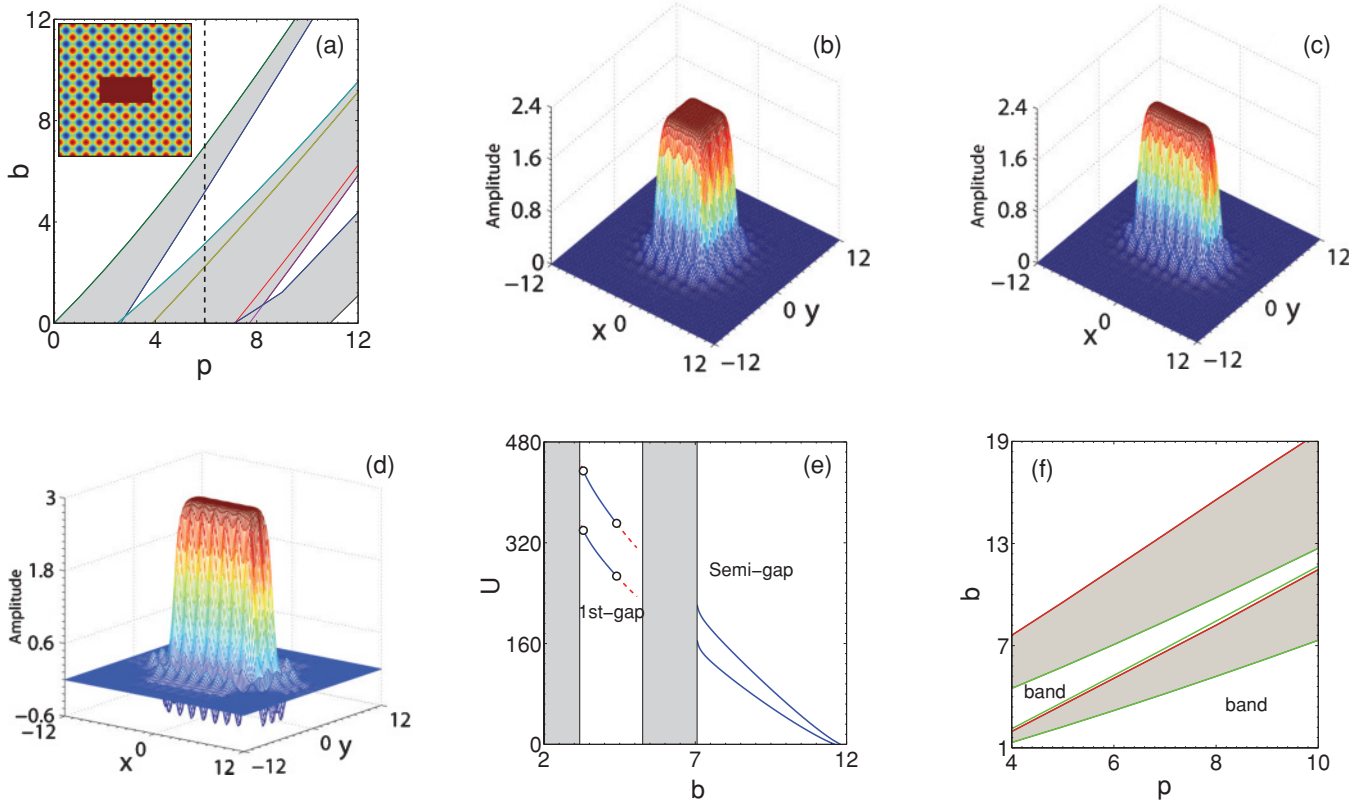

FIG. 1. (Color online) (a) Band-gap structure of a harmonic lattice. Inset: Example of a defective lattice. Profiles of fundamental and higher order nonlinear modes at $b = 7.5, n_{x,y} = 4$ (b), $b = 7.5, n_x = 6, n_y = 2$ (c) in the semi-infinite gap and $b = 4.0, n_x = 6, n_y = 2$ (d) in the first-finite gap. (e) Energy flow versus b for $n_{x,y} = 4$ (upper) and $n_x = 6, n_y = 2$ (lower). Dashed curves denote the unstable solitons. (f) Existence regions (shaded) on the (p,b) plane for $n_x = 4, n_y = 2$, green lines (online) show the gap edges. All quantities are plotted in arbitrary dimensionless units.

a partially spatially incoherent optical beam [18]. Another technique is to introduce partial incoherence into the lattice beam by letting the lattice beam go through a rotating diffuser. This partial incoherence reduces the nonlinear interference between lattice sites, which stabilizes the lattice and the defect [30]. Equation (1) conserves the energy flow: $U = \int_{-\infty}^{\infty}\int_{-\infty}^{\infty} |q(x,y)|^2 dxdy$.

We search for nonlinear localized modes in the form $q = [w_r(x,y) + iw_i(x,y)]\exp(ibz)$, where w_r and w_i represent the real and imaginary parts of the light field, respectively, and b is the propagation constant. The topological winding number (or topological charge) of the vortex soliton is obtained as the circulation of the phase gradient $\arctan(w_i/w_r)$ around a phase singularity located in the vicinity of the vortex core. The stationary solutions were solved numerically by a relaxation method. To study the linear stability, we consider the evolution of small-amplitude perturbations of the localized state presenting the solution in the form $q = (w_r + iw_i + u_r + iu_i)\exp(ibz)$ and assume $u_{r,i} \sim \exp(\lambda z)$. Thus, the evolution of the perturbation is determined by

$$\lambda u_i = \tfrac{1}{2}\Delta u_r - \left(3w_r^2 + w_i^2\right)u_r - 2w_r w_i u_i - bu_r + pRu_r, \tag{2}$$

$$-\lambda u_r = \tfrac{1}{2}\Delta u_i - \left(w_r^2 + 3w_i^2\right)u_i - 2w_r w_i u_r - bu_i + pRu_i. \tag{3}$$

We can obtain the linear eigenvalue problem for $u_{r,i}$, which is used to determine the possible eigenvalues λ. To elucidate the influence of lattice defects on the solitons, we set, unless stated otherwise, $\Omega = 2, p = 6$, $\gamma = 2p$ (for flat-topped defects), $\gamma = 2.5p$ (for attractive defects), $\gamma = 1.5p$ (for repulsive defects), and vary the parameters n_x, n_y, and b.

III. SOLITONS IN LATTICES WITH FLAT-TOPPED DEFECTS

It is instructive to consider the Floquet-Bloch spectrum of the nondefective lattice. The band-gap structure of the linear version of Eq. (1) with $R(x,y) = \cos^2(\Omega x) + \cos^2(\Omega y)$ is shown in Fig. 1(a). The finite gaps expand with the lattice depth. For the purpose of illustration, we only discuss the properties of defect solitons in the semi-infinite and first-finite gap. The inset plot in Fig. 1(a) shows an example of a defective lattice with a flat-topped defect covering several lattice sites with different transverse sizes. Special attention should be paid to the shapes of the solitons shown in Figs. 1(b) to 1(d). The solitons in the semi-infinite gap with $n_{x,y} = 4$ exhibit square amplitude distributions with lower lobes surrounding them [Fig. 1(b)].

When the defect shape is rectangular, the solitons exhibit similar intensity distributions [Fig. 1c] according to the shapes of defects which are very different from conventional solitons

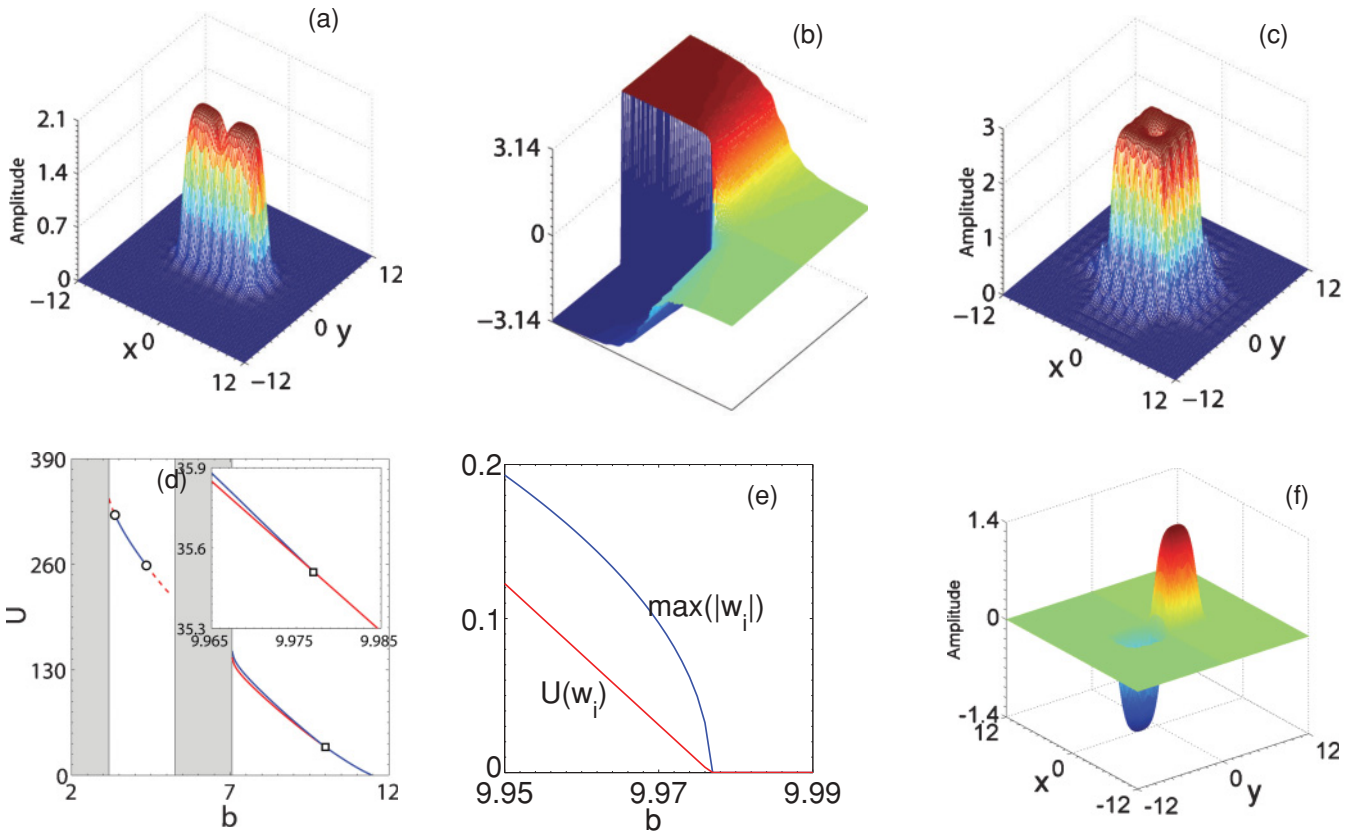

FIG. 2. (Color online) (a), (b) Amplitude and noncanonical phase structure of vortex soliton at $b = 8.0$ in the semi-infinite gap. (c) Amplitude of vortex soliton at $b = 4.0, n_{x,y} = 4$ in the first-finite gap. (d) Energy flow versus b. Dashed curves in the first-finite gap denote the unstable vortex solitons. In the semi-infinite gap, power of both dipole (red) and vortex (blue) solitons are displayed and the square stands for the bifurcation point below which vortex and dipole solitons can be found simultaneously. (e) Energy flow and maximum amplitude of w_i near the break point. (f) Profile of vortex-dipole soliton at $b = 9.977$. Except for (c), $n_x = 6, n_y = 2$. All quantities are plotted in arbitrary dimensionless units.

whose shapes have some types of symmetries. This offers an effective way to control the soliton shape by varying the defect shape. In contrast to the case of completely periodic lattices [4], solitons in defective lattices expand to the outer lattice sites only when the propagation constant approaches the upper band edges. Comparing soliton profiles in the semi-infinite gap with those in the first-finite gap, one immediately finds that solitons residing in the semi-infinite gap belong to the fundamental families since there are no nodes in their amplitudes, but higher order ones in the first-finite gap.

The energy flow of solitons in both semi-infinite and first-finite gaps decreases with the propagation constant [Fig. 1(e)]. It is enhanced greatly compared with nondefective lattices because of a higher refractive-index core. In the semi-infinite gap, energy flow vanishes when the propagation constant exceeds a critical cutoff value. Solitons in the first-finite gap cease to exist when the propagation constant approaches the lower edge of the first band. The upper propagation-constant cutoffs of solitons in the semi-infinite gap grow linearly with the lattice depth while the existence domains expand just like the gap structure of the lattice. The existence domains of fundamental and higher order solitons are presented in Fig. 1(f).

In order to determine the linear stability properties of defective lattice solitons, we numerically solved in an exhaustive manner the eigenvalue problems for various families of solitons based on Eq. (2). For fundamental solitons in the semi-infinite gap, we did not find any eigenvalues with nonzero real parts. Thus, solitons are stable in their entire existence domain. This result is in good agreement with the prediction from the Vakhitov-Kolokolov (VK) criterion ($dU/db < 0$ for defocusing nonlinearity). However, the higher order solitons suffer from weak instability when the propagation constant approaches the upper edge of the first-finite gap. There also exists a very narrow instability region near the lower edge of the first-finite gap [see the dashed curve in Fig. 1(e)].

We stress that, contrary to the fact that vortex solitons in defocusing nonlinear media with imprinted periodic lattices can only be found in finite gaps, we found vortex-soliton solutions in the semi-infinite gap [Figs. 2(a) and 2(b)]. Typical examples of vortex solutions with unit charge supported by defective lattices in the semi-infinite and first-finite gaps are displayed in Fig. 2. Unlike in canonical radially symmetric vortices featuring constant phase gradients $d\theta/d\phi$ (here θ is the vortex phase and ϕ is the azimuthal angle), for our vortices $d\theta/d\phi$ is azimuthally dependent [Figs. 2(b) and 7(e)]. The phase increases most rapidly around $\phi = \pi/2$ and $3\pi/2$, while $d\theta/d\phi$ is minimal in the vicinity of the intensity maxima. It

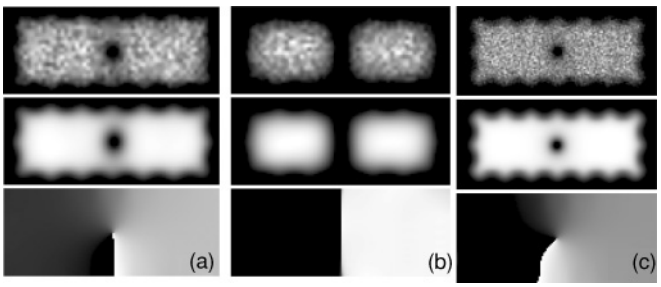

FIG. 3. Stable propagation of vortex solitons (a), (c) and dipole soliton (b) in the semi-infinite gap (a), (b) and first-finite gap (c) at $n_x = 6, n_y = 2$. (a) $b = 7.5$. (b) $b = 10.0$. (c) $b = 4.0$. Top rows: $z = 0$. Middle rows: $z = 512$. Bottom rows: phase structures at $z = 512$. White noise was added into the initial inputs.

is similar to the noncanonical phase structure of the surface vortex soliton reported in [31].

Similar to fundamental solitons, the profiles of vortex solitons are very steep and the energy flow is a decreasing function of the propagation constant. A stability analysis based on Eq. (2) indicates that vortex and dipole solitons in the semi-infinite gap are completely stable in their existence domains. Vortex solitons in the first-finite gap are stable in a relatively wide parameter window when the propagation constant resides on the solid lines [Fig. 2(d)]. Surprisingly, vortex solutions stop existing at $b = 9.977$, above which only dipole solutions can be found. This result can be attributed to the bifurcation that occurs at this point. The power of two branches of solitons (dipole and vortex) converges to a collective curve when the propagation constant approaches the critical value. The bifurcation does not occur for fundamental solitons in rectangular defects and vortex solitons in square defects. To clarify the disappearance of vortex solitons and the emergence of dipole solitons more clearly, we plot in Fig. 2(e) the maximum amplitude of the imaginary parts of soliton solutions $\max(|w_i|)$ and their "power" near the break point of the propagation constant. One can see that the imaginary part of the stationary solution disappears when the propagation constant exceeds the critical value. The profile of a vortex-dipole soliton at $b = 9.977$ is displayed in Fig. 2(f). Note that a similar bifurcation also occurs for elliptic vortices trapped in composite Mathieu lattices [32] and self-attractive Bose-Einstein condensates [33].

To verify the linear stability results, we checked the robustness of nonlinear states by using the split-step Fourier method and by adding random noise on both the amplitude and phase. Figure 3 presents some examples of stable propagation of dipole and vortex solitons residing in both the semi-infinite gap and first-finite gap supported by flat-topped defects. The strong noise added to the initial input beams soon radiates away and the phase structures of vortex solitons go back to those of unperturbed solitons after a short propagation distance.

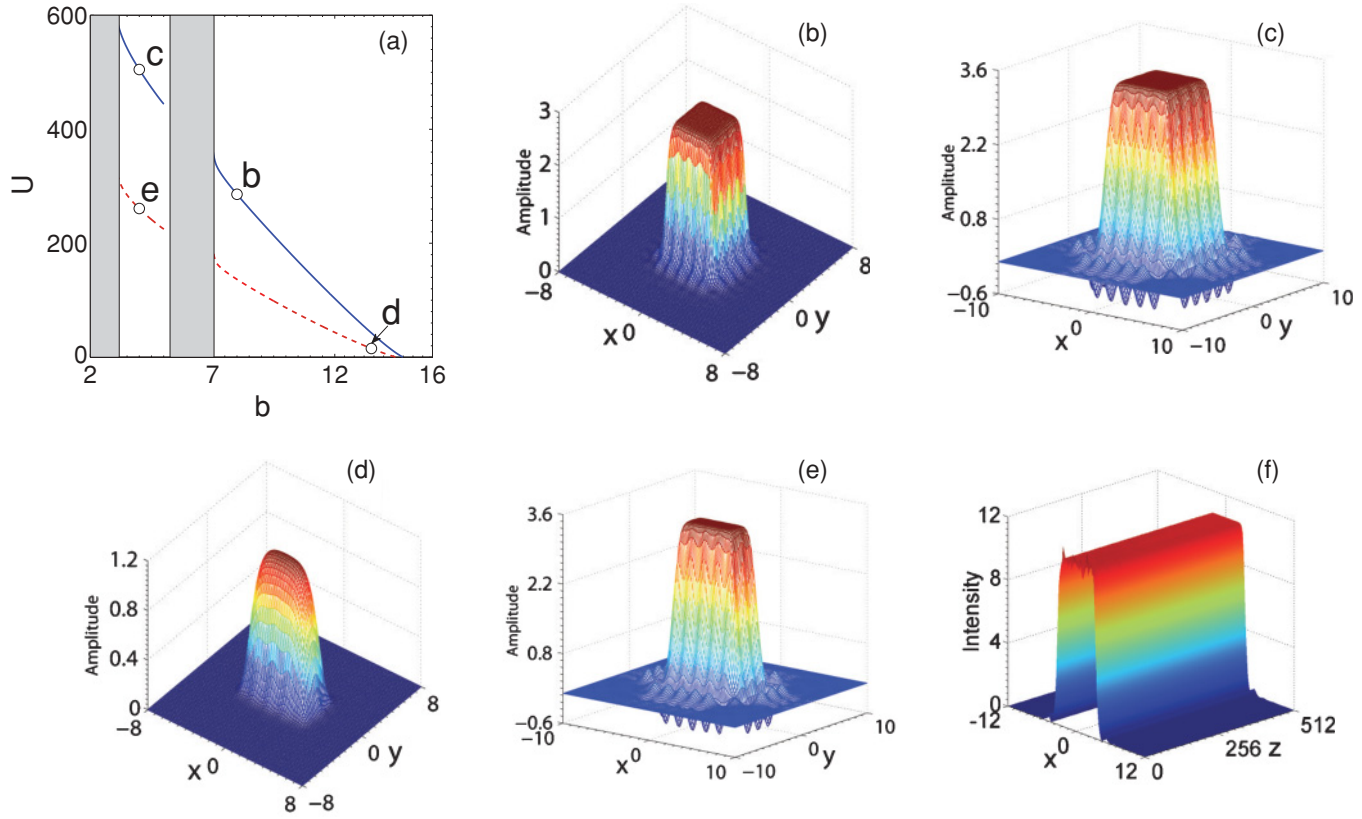

FIG. 4. (Color online) Defect fundamental solitons in the semi-infinite gap and higher order solitons in the first-finite gap for the attractive defect with $n_{x,y} = 4$ and $n_x = 4$, $n_y = 2$ [dashed in (a)]. (a) Power diagram. (b)–(e) profiles of four defect solitons at $b = 8$, 4, 13.5, and 4 [marked by circles in (a)], respectively. (e) Stable propagation of soliton at $b = 4.4$ in the defect with $n_{x,y} = 4$. Cut of intensity distribution at $y = 0$ is shown. All quantities are plotted in arbitrary dimensionless units.

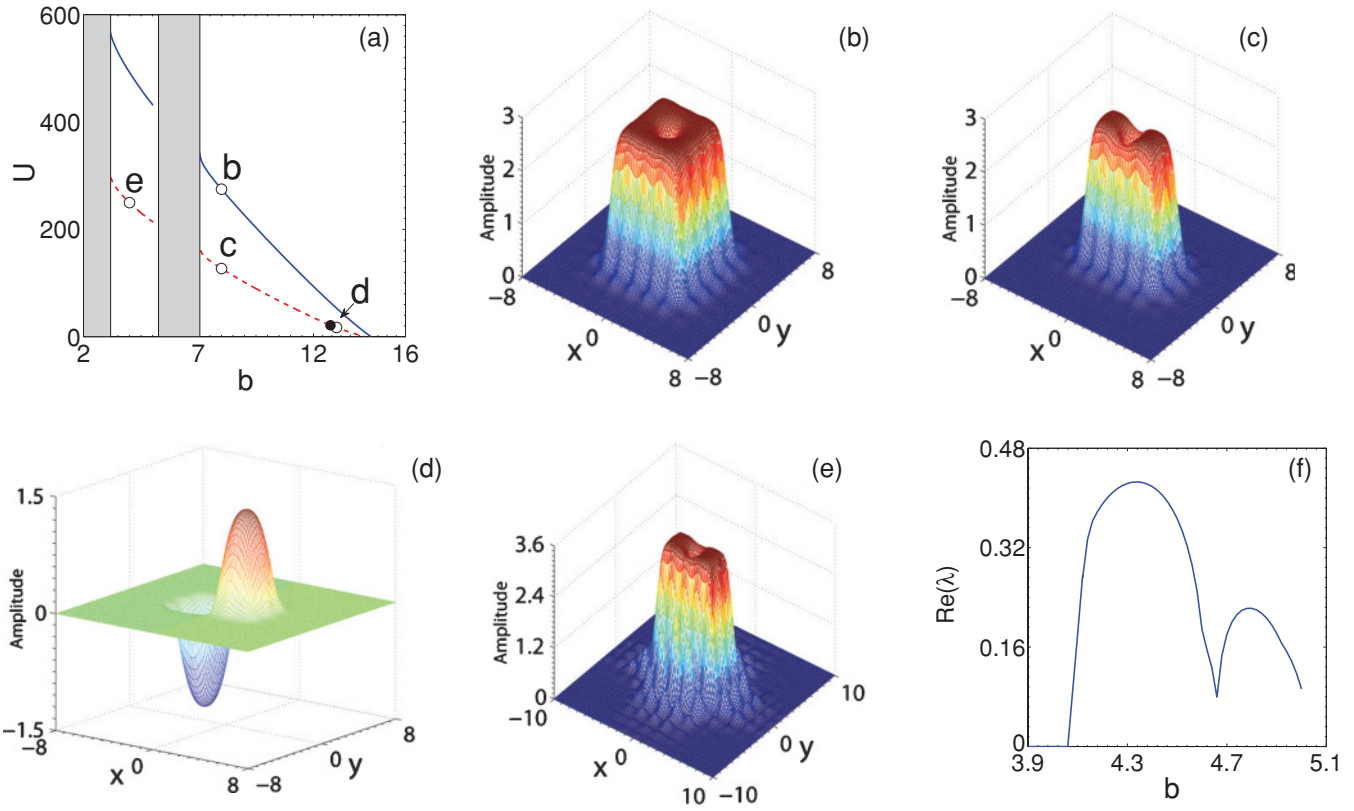

FIG. 5. (Color online) Defect vortex solitons in the attractive defect with $n_{x,y} = 4$ and $n_x = 4$, $n_y = 2$ [dashed in (a)]. (a) Power diagram. Black point divides the stable vortex and dipole solitons. (b)–(e) Profiles of four defect solitons at $b = 8$, 8, 13, and 4 [marked by circles in (a)], respectively. (e) Instability growth rate of defect vortex solitons. All quantities are plotted in arbitrary dimensionless units.

IV. SOLITONS IN LATTICES WITH ATTRACTIVE AND REPULSIVE DEFECTS

We now consider the properties of solitons supported by attractive defective lattices. The energy flow of solitons in both gaps still decreases with the growth of propagation constant due to the defocusing nonlinearity [Fig. 4(a). However, the existence domains of solitons in the semi-infinite gap are broader than those of flat-topped-defect solitons [Fig. 1(e)]. The energy flows are larger than those of flat-topped-defect solitons. The results should be attributed to the higher refractive-index core.

Representative examples of soliton profiles are depicted in Fig. 4. In the semi-infinite gap, the maximum amplitude slowly grows with decreasing propagation constant and the small lobes do not expand in an obvious manner to outside lattice sites. When the propagation constant approaches the cutoff value, the soliton no longer maintains its square or rectangular distribution [Fig. 4(d)]. The higher order soliton solutions in the first-finite gap gradually delocalize when the propagation constant decreases. However, the process of delocalization is apparently slower than in the 1D case [20] due to the strong trapping ability of the large-scale lattice defect. The stable regions are slightly broader than that of flat-topped defects due to the higher index core. Figure 4(f) displays an example of the stable propagation of a higher order soliton at $b = 4.4$ in the first-finite gap while the corresponding soliton in the flat-topped defect is unstable.

In the semi-infinite gap, vortex solitons were also found in attractive defects. For $n_{x,y} = 4$, the vortex has a square structure with a dark intensity core. The amplitude distributions of vortex solitons maintain their shapes and the amplitude maxima decrease slowly with growing propagation constant. The phase carries a linear screw-type dislocation around the dark core, just like for bulk media or nondefective harmonic lattices.

However, for vortex solitons in defects with different transverse sizes (e.g., $n_x = 4, n_y = 2$), the phase variation around the dislocation does not increase uniformly [see also Fig. 2(b)]. Moreover, two amplitude minima exist in the vortices in the narrower defect direction [Fig. 5(c)]. The minima decrease gradually with propagation constant and the vortices break into dipoles when the propagation constant exceeds a critical value ($b_{cr} = 12.732$). Accordingly, the phase changes from a nonuniform stair-like structure to a step-jump structure. We proved that the dipoles are actual dipole solitons since they are nonlinear modes and can propagate stably with two out-of-phase components [Fig. 5(d)]. In other words, each component of the dipole cannot be a self-localized entity alone and only two components together can be guided stably by the defective lattices [Fig. 3(b)]. Vortex solitons in the first-finite gap [Fig. 5(e)] contain higher amplitude maxima and side lobes than in the semi-infinite gap. The delocalization occurs when the propagation constant approaches the lower edge of the gap. The instability growth rate of vortex solitons in the defect with $n_x = 4, n_y = 2$ is shown in Fig. 5(f). Obviously, vortex

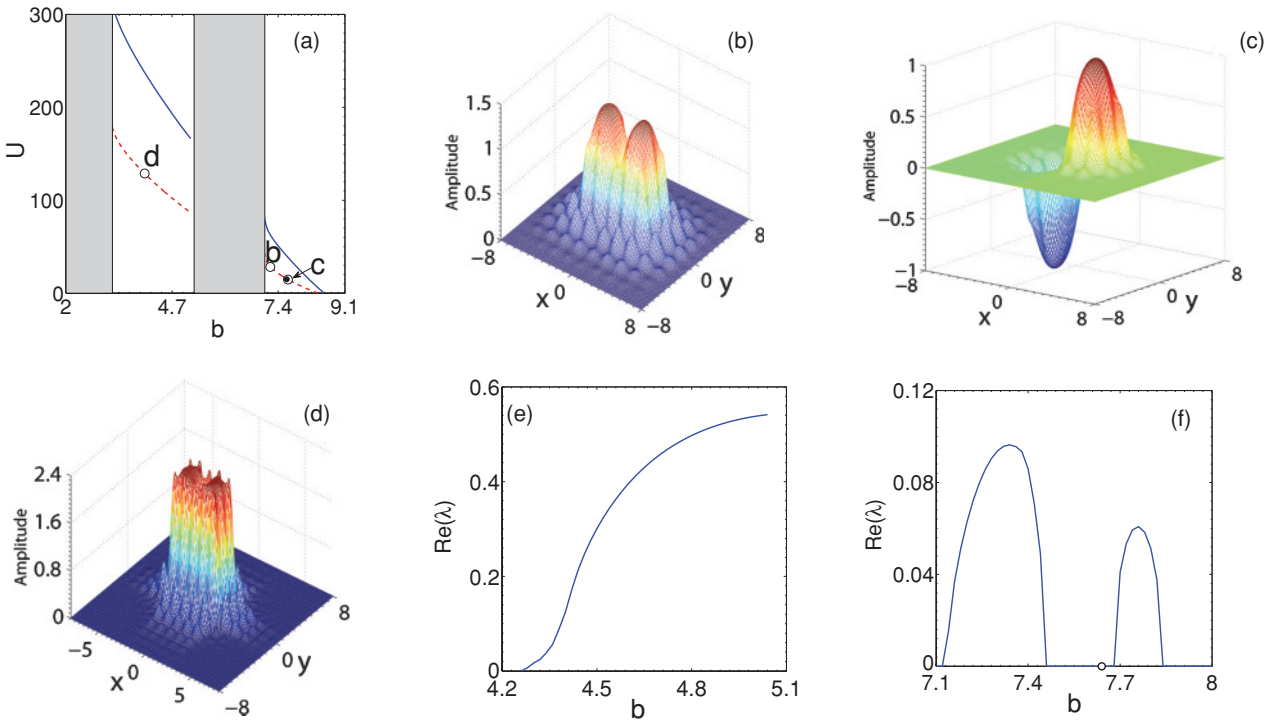

FIG. 6. (Color online) Defect vortex solitons in the repulsive defect with $n_{x,y} = 4$ and $n_x = 4$, $n_y = 2$ [dashed in (a)]. (a) Power diagram. Black point [corresponding to the circle in (f)] divides the vortex and dipole solitons. (b)–(d) Profiles of three defect solitons at $b = 7.2$, 7.65, and 4 [marked by circles in (a)], respectively. Instability growth rate of defect vortex solitons in the first-finite gap (e) and vortex-dipole solitons in the semi-infinite gap (f). All quantities are plotted in arbitrary dimensionless units.

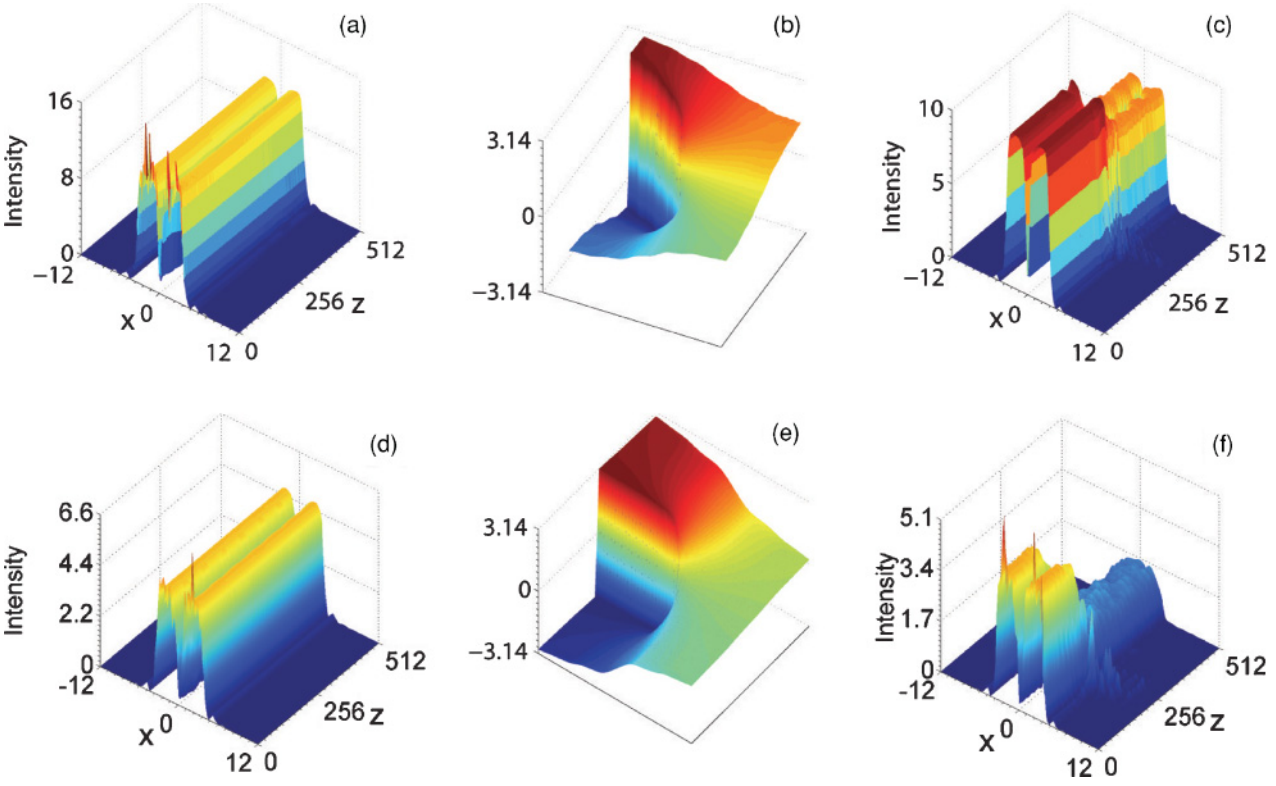

FIG. 7. (Color online) Stable and unstable propagation of vortex solitons in the first-finite gap of attractive (a)–(c) and repulsive (d)–(f) defective lattices. $b = 3.32$ in (a) and (b), 4.4 in (c), 4.2 in (d) and (e), and 4.5 in (f). (b), (e) Phase distributions of solitons shown in (a) and (d) at $z = 512$. Cut of intensity distributions at $y = 0$ are shown. Top row: $n_{x,y} = 4$. Bottom row: $n_x = 4, n_y = 2$. All quantities are plotted in arbitrary dimensionless units.

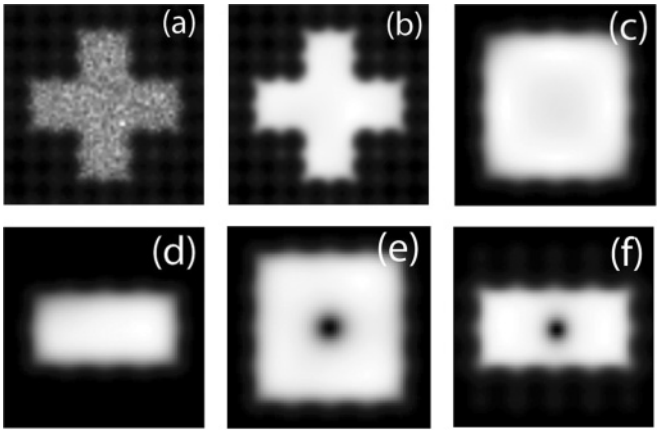

FIG. 8. Propagation simulation of an example of cruciform solitons at $z = 0$ (a) and 512 (b) respectively. (c), (d) Propagation results of a Gaussian beam in the form $w_r = 4\exp[-(x^2 + y^2)/25]$ at $z = 800$. (e), (f) Propagation results of a beam in the form $w = 4\exp[-(x^2 + y^2)/25]\exp(i\phi)$ at $z = 400$. (c), (e) $n_{x,y} = 4$. (d), (f) $n_x = 4, n_y = 2$. $\gamma = 2p$ in (a) and (b) and $2.5p$ in (c)–(f). White noise was added into the initial inputs.

solitons in the first-finite gap are stable over a relatively wide window. Note that there also exists a very narrow instability region near the lower edge of the first-finite gap, just similar to the vortex solitons in flat-topped defects.

The properties of solitons in the repulsive defective lattices are qualitatively similar to those in the flat-topped and attractive defective lattices. We only make four comments here. First, both fundamental and vortex solitons can still be found in the semi-infinite gap. The existence domains of (vortex) solitons shrink in comparison with the flat-topped and attractive defective lattices [Fig. 6(a)]. We expect that there exists a critical $\gamma_{\rm cr}$ below which no fundamental or vortex soliton can be found in the semi-infinite gap. This is in agreement with the 1D case in repulsive defective lattices [20]. Second, the vortex solitons in the defect with $n_x = 4$ and $n_y = 2$ also break into dipole solitons at $b_{\rm cr} = 7.611$ while the fundamental solitons with $n_{x,y} = 4$ and $n_x = 4, n_y = 2$ and vortex solitons with $n_{x,y} = 4$ do not break [Fig. 6(c)]. The two minima of vortex solitons connecting the two central main lobes are lower than that for flat-topped and attractive defects [Fig. 6(b)]. The profile and phase distributions of vortex solitons in the semi-infinite gap are similar to the azimuthons proposed by Desyatnikov *et al.* [34]. Third, the profiles of vortices in the first-finite gap have several discrete peaks around the edges of the square or rectangular defect since the lattice intensities at these peaks are higher than the repulsive defect [Fig. 6(d)]. The delocalization process of solitons is faster than that in the flat-topped and attractive defects due to the lower refractive-index core. Finally, propagation simulations reveal that fundamental solitons in the semi-infinite gap suffer weak oscillatory instability for certain propagation-constant windows, which indicates that the VK criterion fails to predict the instability of fundamental solitons in repulsive defects. Linear stability analysis results of vortex-dipole solitons in the repulsive defect with $n_x = 4, n_y = 2$ are shown in Figs. 6(e) (first-finite gap) and 6(f) (semi-infinite gap), respectively. Figure 7 presents some stable and unstable propagations of vortex solitons in the attractive and repulsive defect. Figures 7(b) and 7(e) illustrate again the difference between the canonical and noncanonical phase structures.

For a deeper insight into the guiding effect of the defective lattice, we change the defect shape to study the properties of solitons. A typically stable propagation example of cruciform solitons supported by a lattice with a cruciform flat-topped defect is presented in Figs. 8(a) and 8(b). Lattice defects with other shapes may lead to the formation of more complicated structures. In experiments, the probe beams used to excite solitons are usually Gaussian beams. Thus, the evolution of a Gaussian beam guided by the defective lattice is important. We input a Gaussian beam in the form $w_r = 4\exp[-(x^2 + y^2)/25]$ and monitor its evolution in the defective lattices. Figures 8(c) and 8(d) show the propagation results of the Gaussian beam after a very long distance. We can see that solitons with square or rectangular shapes can be formed in the defective lattices with corresponding defect shapes. For the realization of vortex solitons, one can add a vortex phase mask before the input Gaussian beam. Examples of excitations of vortex solitons in defective lattices in the form $w = 4\exp[-(x^2 + y^2)/25]\exp(i\phi)$ are presented in Figs. 8(e) and 8(f). The phase structures of the fields at $z = 400$ are similar to those displayed in Figs. 7(b) and 7(e). We also simulate the evolution of solitons and Gaussian beams by removing the self-defocusing nonlinearity. No stable localized patterns are found, which indicates that the defocusing nonlinearity is a necessary ingredient for the existence of stable solitons.

V. CONCLUSIONS

To summarize, we propose a regime that consists of an optical lattice with a flat-topped refractive-index defect covering several lattice sites for supporting localized nonlinear modes, including fundamental, dipole, and vortex solitons. We show that the soliton shape can be conveniently controlled by properly selecting defects with a similar shape in periodic lattices. Properties of solitons in attractive and repulsive defective lattices are also discussed. We conclude that stable defect solitons in defocusing media can exist in the semi-infinite gap and even in repulsive defects provided that the defect is not very deep. The possibilities of their existences can be accounted for by their associated refractive-index changes. In particular, we find that stable vortex solitons with an nonconventional intensity and phase distribution can be supported by defects with different transverse sizes. Our findings can be applied directly to Bose-Einstein condensates with repulsive interactions in 2D defective lattices.

ACKNOWLEDGMENTS

The authors are indebted to Dr. Jiandong Wang for useful discussions. This work is supported by the National Natural Science Foundation of China (Grant No. 10704067) and Natural Science Foundation of Zhejiang Province, China (Grant No Y6100381).

[1] Y. S. Kivshar and G. P. Agrawal, *Optical Solitons: from Fibers to Photonic Crystals* (Academic, San Diego, 2003).
[2] J. W. Fleischer, M. Segev, N. K. Efremidis, and D. N. Christodoulides, Nature (London) **422**, 147 (2003).
[3] D. N. Christodoulides, F. Lederer, and Y. Silberberg, Nature (London) **424**, 817 (2003).
[4] J. Yang and Z. H. Musslimani, Opt. Lett. **28**, 2094 (2003).
[5] J. Yang, I. Makasyuk, A. Bezryadina, and Z. Chen, Opt. Lett. **29**, 1662 (2004).
[6] J. Yang, I. Makasyuk, A. Bezryadina, and Z. Chen, Stud. Appl. Math. **113**, 389 (2004).
[7] J. Yang, New J. Phys. **6**, 47 (2004).
[8] D. N. Neshev, T. J. Alexander, E. A. Ostrovskaya, Y. S. Kivshar, H. Martin, I. Makasyuk, and Z. Chen, Phys. Rev. Lett. **92**, 123903 (2004).
[9] J. W. Fleischer, G. Bartal, O. Cohen, O. Manela, M. Segev, J. Hudock, and D. N. Christodoulides, Phys. Rev. Lett. **92**, 123904 (2004).
[10] M. I. Rodas-Verde, H. Michinel, and Y. S. Kivshar, Opt. Lett. **31**, 607 (2006).
[11] A. S. Desyatnikov, Yu. S. Kivshar, and L. Torner, *Optical Vortices and Vortex Solitons*, Prog. Opt. 47, edited by E. Wolf (North-Holland, Amsterdam, 2005), pp. 291–391.
[12] J. Yang, I. Makasyuk, P. G. Kevrekidis, H. Martin, B. A. Malomed, D. J. Frantzeskakis, and Z. Chen, Phys. Rev. Lett. **94**, 113902 (2005).
[13] C. Lou, X. Wang, J. Xu, Z. Chen, and J. Yang, Phys. Rev. Lett. **98**, 213903 (2007).
[14] M. G. Clerc, F. Haudin, S. Residori, U. Bortolozzo, and R. G. Rojas, Eur. Phys. J. D **59**, 43 (2010).
[15] F. Fedele, J. Yang, and Z. Chen, Opt. Lett. **30**, 1506 (2005).
[16] X. Wang, J. Young, Z. Chen, D. Weinstein, and J. Yang, Opt. Express **14**, 7362 (2006).
[17] J. Wang, J. Yang, and Z. Chen, Phys. Rev. A **76**, 013828 (2007).
[18] I. Makasyuk, Z. Chen, and J. Yang, Phys. Rev. Lett. **96**, 223903 (2006).
[19] K. B. Dossou, L. C. Botten, R. C. McPhedran, C. G. Poulton, A. A. Asatryan, and C. Martijn de Sterke, Phys. Rev. A **77**, 063839 (2008).
[20] J. Yang and Z. Chen, Phys. Rev. E **73**, 026609 (2006).
[21] R. Wang, C. Zhang, L. Kong, and Y. Zhang, Opt. Commun. **281**, 4509 (2008).
[22] W. H. Chen, Y. J. He, and H. Z. Wang, Opt. Express **14**, 11271 (2006).
[23] Y. Li, W. Pang, Y. Chen, Z. Yu, J. Zhou, and H. Zhang, Phys. Rev. A **80**, 043824 (2009).
[24] A. Szameit, Y. V. Kartashov, M. Heinrich, F. Dreisow, T. Pertsch, S. Nolte, A. Tünnermann, F. Lederer, V. A. Vysloukh, and L. Torner, Opt. Lett. **34**, 797 (2009).
[25] W. H. Chen, X. Zhu, T. W. Wu, and R. H. Li, Opt. Express **18**, 10956 (2010).
[26] M. J. Ablowitz, B. Ilan, E. Schonbrun, and R. Piestun, Phys. Rev. E **74**, 035601 (2006).
[27] F. Ye, Y. V. Kartashov, V. A. Vysloukh, and L. Torner, Opt. Lett. **33**, 1288 (2008).
[28] F. Ye, Y. V. Kartashov, V. A. Vysloukh, and L. Torner, Phys. Rev. A **78**, 013847 (2008).
[29] G. Bartal, O. Cohen, H. Buljan, J. W. Fleischer, O. Manela, and M. Segev, Phys. Rev. Lett. **94**, 163902 (2005).
[30] Z. Chen and J. Yang, *Optically-Induced Reconfigurable Photonic Lattices for Linear and Nonlinear Control of Light*, Nonlinear Optics and Applications, edited by H. A. Abdeldayem and D. O. Frazier (India, Kerala, 2007), pp. 103–149.
[31] Y. V. Kartashov, A. A. Egorov, V. A. Vysloukh, and L. Torner, Opt. Express **14**, 4049 (2006).
[32] F. Ye, D. Mihalache, and B. Hu, Phys. Rev. A **79**, 053852 (2009).
[33] F. Ye, L. Dong, B. A. Malomed, D. Mihalache, and B. Hu, J. Opt. Soc. Am. B **27**, 757 (2010).
[34] A. S. Desyatnikov, A. A. Sukhorukov, and Y. S. Kivshar, Phys. Rev. Lett. **95**, 203904 (2005).